A Family of Converters for UPS Production Burn-In Energy Recovery

Carlos Augusto Ayres, *Student Member, IEEE,* and Ivo Barbi, *Senior Member, IEEE*

***Abstract*—This paper introduces a family of power converters for power recycling during the burn-in test of synchronized uninterruptible power supplies (UPS's) with sinusoidal output voltage.**

The use of the power recycler to replace the resistor load bank in the UPS's burn-in test causes great energy savings, and the optimized use of electrical energy contributes in reducing the final cost of the product.

The main feature of the new circuits is their ability to draw from the UPS and to inject into the utility-grid currents with low total harmonic distortion (THD) and high power factor (PF).

The new circuits operate at constant frequency and are regulated by conventional pulse width modulation (PWM) using dedicated PWM and PF controller integrated circuits developed for power supplies.

Circuit operation, mathematical analysis, design example, and experimental results for discontinuous current mode (DCM) and continuous current mode (CCM) operation are provided in this paper.

***Index Terms*—Inverters, power-factor correction, rectifiers, uninterruptible power supply.**

I. Introduction

USUALLY, in burn-in tests of uninterruptible power supplies (UPS's), the manufacturers use resistors as a load, which presents large energy losses and contributes in increasing the cost of the final product.

Methods to feed this energy back into the utility have been proposed in recent literature.

In [1] and [2], a technique, which uses power converters, is presented, and the corresponding block diagram is shown in Fig. 1. The inverter bridge of the dc power recycler is modulated to impose a sinusoidal output current so that a low total harmonic distortion (THD) current is injected into the utility. This technique, therefore, requires an active control of the ac inverter current, which needs complex circuitry. Besides, the low-frequency transformers (TR's) are necessary to adapt the voltages to ensure the correct operation of the inverter, and the bulky capacitors C_F must be used to filter the rectified voltage at the dc link.

In [3], the quadrature voltage injection is used to transfer power from the UPS to the utility. The injected voltage can be obtained by using two autotransformers or a controlled voltage inverter. Fig. 2 illustrates the block diagram for this proposal.

In [4], the proposal consists of using a regulating transformer and a variable inductance between the UPS under test and the utility grid. This method uses only passive and heavy equipment not suitable for automation of the test procedures. Fig. 3 shows the equivalent circuit diagram for this case.

A different technique [5], [6] intended to be used in the burn-in test of synchronized UPS's is presented in this paper, which is described and studied hereafter.

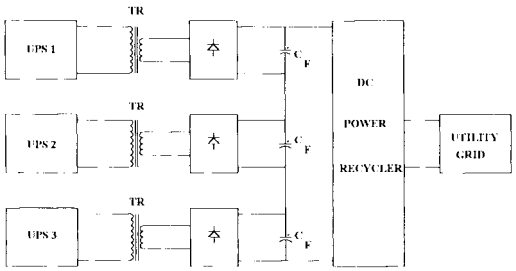

Fig. 1. Block diagram of proposal in [1] and [2].

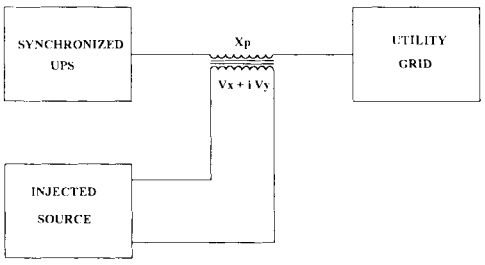

Fig. 2. Block diagram of proposal in [3].

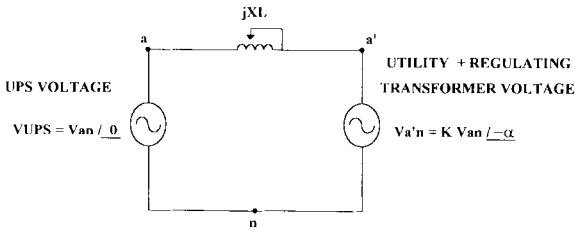

Fig. 3. Equivalent circuit diagram of proposal in [4].

II. The Proposed Power Recycler

Fig. 4 shows the structure of the power recycler for the burn-in test of a synchronized UPS with sinusoidal output

Manuscript received November 6, 1995; revised September 19, 1996. Recommended by Associate Editor, P. N. Enjeti.

C. A. Ayres is with the Department of Electronics, Federal Engineering School of Itajubá, 37500-000, Itajubá, MG Brazil (e-mail: eel1caa@inep.ufsc.br).

I. Barbi is with the Power Electronics Institute, Federal University of Santa Catarina, 88010-970, Florianópolis, SC Brazil (e-mail: ivo@inep.ufsc.br).

Publisher Item Identifier S 0885-8993(97)04988-0.

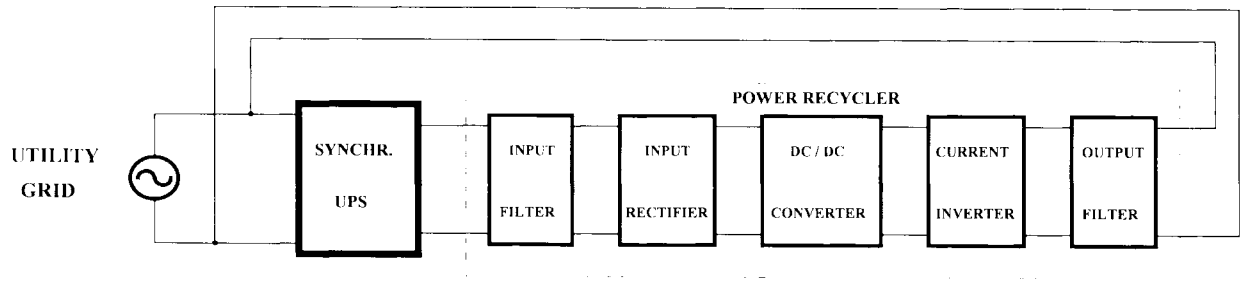

Fig. 4. Proposed structure of the power recycler for the UPS burn-in test.

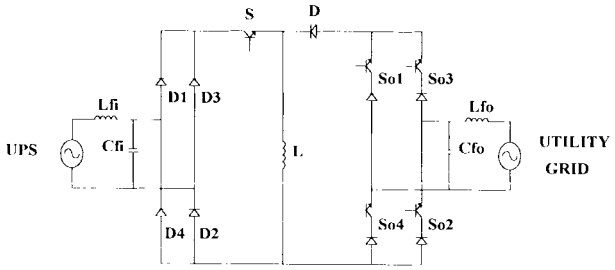

Fig. 5. Power-recycler circuit.

voltage. The first stage of power processing is an input rectifier, resulting in a positive 120-Hz rectified voltage. The second stage is a dc/dc converter. This stage is responsible for imposing a rectified sinusoidal waveform in its input and output current. The last stage is a current inverter, which converts the rectified sinusoidal current from the preceding stage to a sinusoidal current synchronized with the utility grid. The current inverter operates at low frequency, changing the pair of active switches every 120 Hz. As the dc/dc converter introduces high-frequency current harmonics, it is necessary to use filters at the input and output of the structure.

The isolation between the power recycler and utility grid is necessary if the UPS is not isolated. In this case, the isolation can be obtained by using a low-frequency transformer between the power recycler and grid or by using an isolated dc/dc converter.

The dc/dc converter can operate in discontinuous current mode (DCM) or continuous current mode (CCM).

III. DCM Analysis of the Power Recycler

In DCM, we have one interesting characteristic. The semiconductors' current peak naturally follows the sinusoidal waveform of the UPS voltage. So, the power recycler operates in an open loop, and no active control is necessary to obtain a sinusoidal waveform in the UPS-drained and grid-injected currents. According to Fig. 4, every dc/dc converter can be utilized. To describe the operation of the power recycler, the structure with the buck–boost dc/dc converter was used.

Fig. 5 shows the power-recycler circuit using a buck–boost dc/dc converter.

A. Operation Stages

To analyze the operation stages of the power recycler, one can consider that the input and output voltages are constant

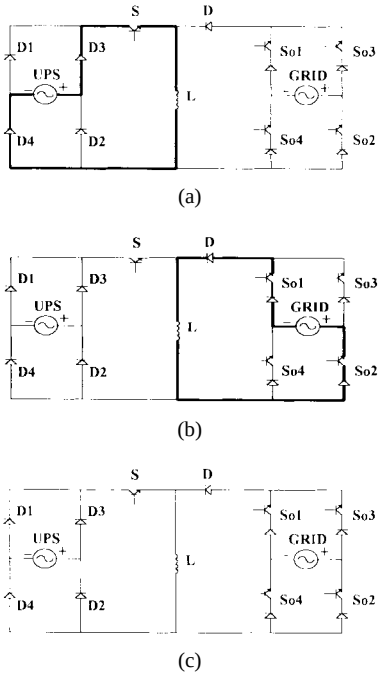

Fig. 6. The stages of operation in DCM for a half period of the grid voltage.

during the switching period since the switching frequency is much higher than the grid frequency. In DCM, there are three stages of operation, which are presented in Fig. 6.

First Stage (t_o–t_1): At instant t_o, switch S is turned on. Diode D is off, and the switch current increases linearly from zero. During this stage, the energy is transferred from the UPS to the buck–boost inductor through the input rectifier. At instant t_1, switch S is turned off, finishing this stage.

Defining the UPS voltage

$$V_i(\theta) = V_{ip} \sin \theta \tag{1}$$

where

V_{ip} UPS voltage peak.

During this interval, the switch and inductor currents are the same and are given in

$$I_L(t) = I_S(t) = \frac{V_{ip} \sin \theta}{L} t \tag{2}$$

$$I_D(t) = 0. \tag{3}$$

Second Stage (t_1–t_2): When switch S is blocked at instant t_1, diode D assumes the inductor current. So, the energy stored in the inductor is transferred to the output through the current

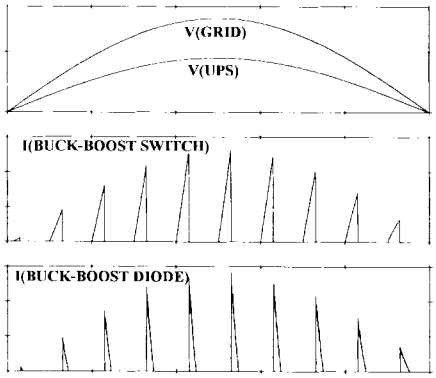

Fig. 7. Main waveforms in a half period of the grid voltage.

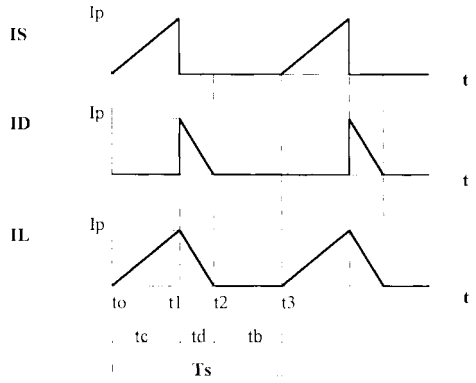

Fig. 8. Main waveforms in a switching period.

inverter. The diode current decreases linearly. At instant t_2, this current reaches zero and the diode blocks, finishing this stage.

The utility voltage is given in

$$V_o(\theta) = V_{op} \sin \theta \tag{4}$$

where

V_{op} utility-voltage peak.

The currents in the diode and the inductor are the same during this interval and are given in

$$I_L(t) = I_D(t) = I_P(\theta) - \frac{V_{op} \sin \theta}{L} t \tag{5}$$

where

$I_p(\theta)$ switch-current peak in angle θ

and

$$I_S(t) = 0. \tag{6}$$

Third Stage (t_2–t_3): During this stage, switch S and diode D are off and no energy is transferred:

$$I_S(t) = I_D(t) = I_L(t) = 0. \tag{7}$$

Fig. 7 illustrates the most relevant waveforms in a half period of grid voltage (a low-switching frequency was used for clarity), and in Fig. 8, one can find the main-current waveforms in a switching period.

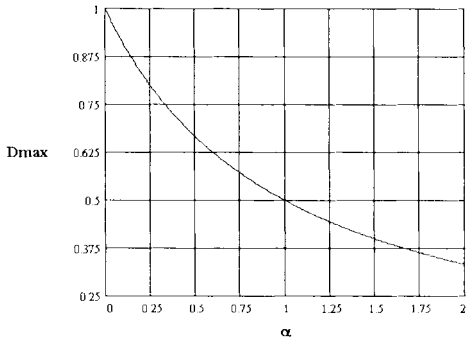

Fig. 9. Maximum duty cycle for DCM operation.

B. Relevant Analysis Results

The most relevant results for DCM are presented hereafter. Defining

T_s switching period;
t_c interval t_0–t_1, where switch S is on;
t_d interval t_1–t_2, where diode D is on;
t_b interval t_2–t_3, where switch S and diode D are off;
D duty cycle.

Using (2) and (5), one can obtain

$$t_d = \alpha t_c = \alpha D_{T_s} \tag{8}$$

where

$$\alpha = \frac{V_{ip}}{V_{op}}. \tag{9}$$

The condition for DCM operation is

$$t_d + t_c \le T_s. \tag{10}$$

The limit for DCM operation imposes a maximum value for the duty cycle

$$D_{\max} \le \frac{1}{1+\alpha}. \tag{11}$$

The curve representing the maximum duty cycle for DCM is plotted in Fig. 9.

The average output current can be obtained by integrating the output current in the switching period and again in a half period of the utility grid

$$\overline{I_{o_{av}}} = \frac{X_L}{V_{op}} I_{o_{av}} = 2\alpha^2 D^2. \tag{12}$$

Using (12), the output characteristic can be expressed in terms of the normalized output power

$$\overline{P_o} = \frac{X_L}{V_{op}^2} P_o = \frac{\pi \alpha^2 D^2}{2}. \tag{13}$$

The normalized inductance can be obtained directly from the normalized output power

$$\overline{X_L} = \frac{P_o}{V_{op}^2} X_L = \frac{\pi \alpha^2 D^2}{2}. \tag{14}$$

Fig. 10 shows the curve of the normalized output power or inductance.

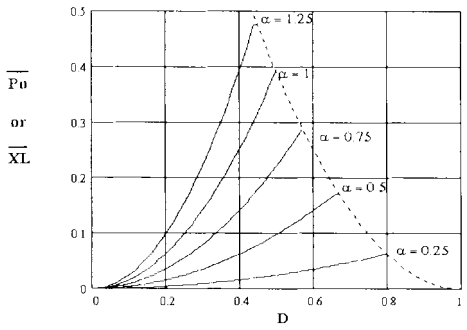

Fig. 10. Normalized output power or inductance.

C. Simplified Design Example

To corroborate the theoretical analysis, a power recycler of 500 W was designed. The characteristics of the converter are

$$V_i = 220\ \mathrm{V_{rms}}\ (60\ \mathrm{Hz})$$
$$V_o = 220\ \mathrm{V_{rms}}\ (60\ \mathrm{Hz})$$
$$P_i = 500\ \mathrm{W}$$
$$f_s = 20\ \mathrm{kHz}.$$

In this case, the value of α is

$$\alpha_{\mathrm{nom}} = 1.$$

Using (11) or Fig. 9, the critical condition is

$$D_{\max} \leq 0.5.$$

To guarantee DCM operation, we chose

$$D = 0.4.$$

Then, the normalized inductance is obtained using (14) or Fig. 10:

$$\overline{X_L} = 0.251 \quad \Rightarrow$$
$$X_L = \frac{V_{op}^2}{P_o}\overline{X_L} = \frac{(220\sqrt{2})^2}{500}\,0.251 = 48.59\ \Omega.$$

Using the switching frequency, the inductance can be calculated

$$L = 387\ \mu\mathrm{H}.$$

The input and output filters are $L_{fi} = L_{fo} = 3.4$ mH and $C_{fi} = C_{fo} = 2\ \mu$F.

As the dc/dc converter has an imposed current, the drive signals of the switches S_{01}/S_{02} and S_{03}/S_{04} can have a small superposition near the zero crossing of the grid voltage. A superposition of 400 μs was used ($\pm 200\ \mu$s around the zero crossing). Then, the current inverter is always enabled. This fact hardly affects the theoretical analysis since, near the zero crossing, the transferred power is low.

D. Experimental Results

A prototype of the 500-W designed power recycler was implemented. The circuit is shown in Fig. 11. One can notice that the position of the buck–boost diode has been changed only for the buck–boost switch to have the same reference as switches S_{01} and S_{03} of the current inverter, but it does not affect the circuit operation. During the experimentation, the UPS was replaced by an isolating transformer. The switches are oversized because the main objective was to prove the operation principle of the converter. Fig. 12 shows the obtained experimental results.

The prototype drained around 572 W from the UPS with a duty cycle of 0.4. The drained power was higher than design, but this can be explained. There is a ripple in the capacitor voltage of the filter, and during most of the conduction time of the buck–boost switch, this voltage is higher than the UPS voltage. So, the current in the buck–boost switch does not have a perfectly triangular waveform. The resulting average value of the buck–boost switch current is a little higher and provokes an increase in the power. The 223-$\mathrm{V_{rms}}$ voltage grid at the moment of acquisition resulted in an increase of 2.75% in the drained power [according to (13)]. Some error due to practical implementation must be considered. The utility voltage presented a THD of 3.34%. The current injected into the utility grid presented a THD of 6.7% and an angle of -7°, resulting in an almost unitary power factor (PF).

The recycled power was 483 W, and the obtained efficiency was 84.4%. The current drained from the UPS also presented a quasi-unitary PF with an angle of $+2.6^\circ$ and a THD of 4.5%. Notice that, in Fig. 12, the current injected into the utility grid was plotted at 180° shifted from the utility voltage because the power flux is from the converter to the grid.

IV. CCM Analysis of the Power Recycler

Though the DCM operation has the advantage of simplicity because it operates in an open loop, the semiconductors are submitted to high-current peaks.

In CCM, a current loop is necessary for obtaining input and output sinusoidal currents, but the semiconductors' current peak is reduced, and the filtering of the high-frequency harmonics of the input and output currents becomes easier. This fact will cause a reduction in the volume of the filters.

Another important characteristic of this operation mode is that if a sinusoidal current is imposed in the dc/dc converter inductor, sinusoidal currents with low THD and high PF are obtained at the power-recycler input and output.

A. Operation Stages

The analysis was done using a buck–boost dc/dc converter. In CCM, there are only two operation stages—basically the same as the two first stages of DCM operation, as illustrated in Fig. 13. The unique difference is that in CCM, the inductor current does not reach zero every switching period. In this case, the semiconductors have a trapezoidal-current waveform instead of a triangular waveform, as shown in Fig. 14.

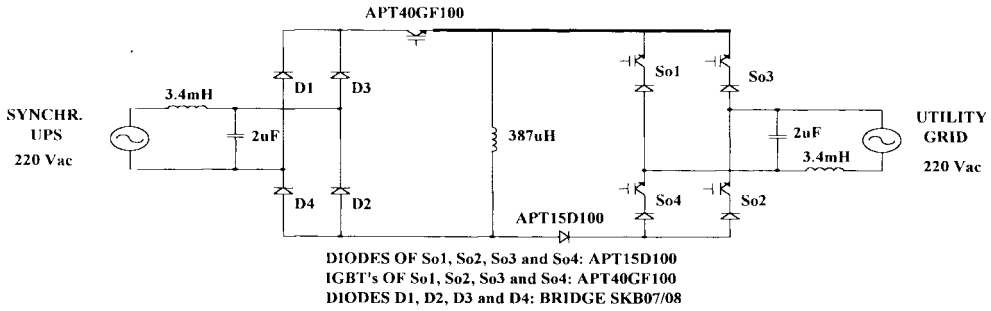

Fig. 11. Implemented circuit for DCM.

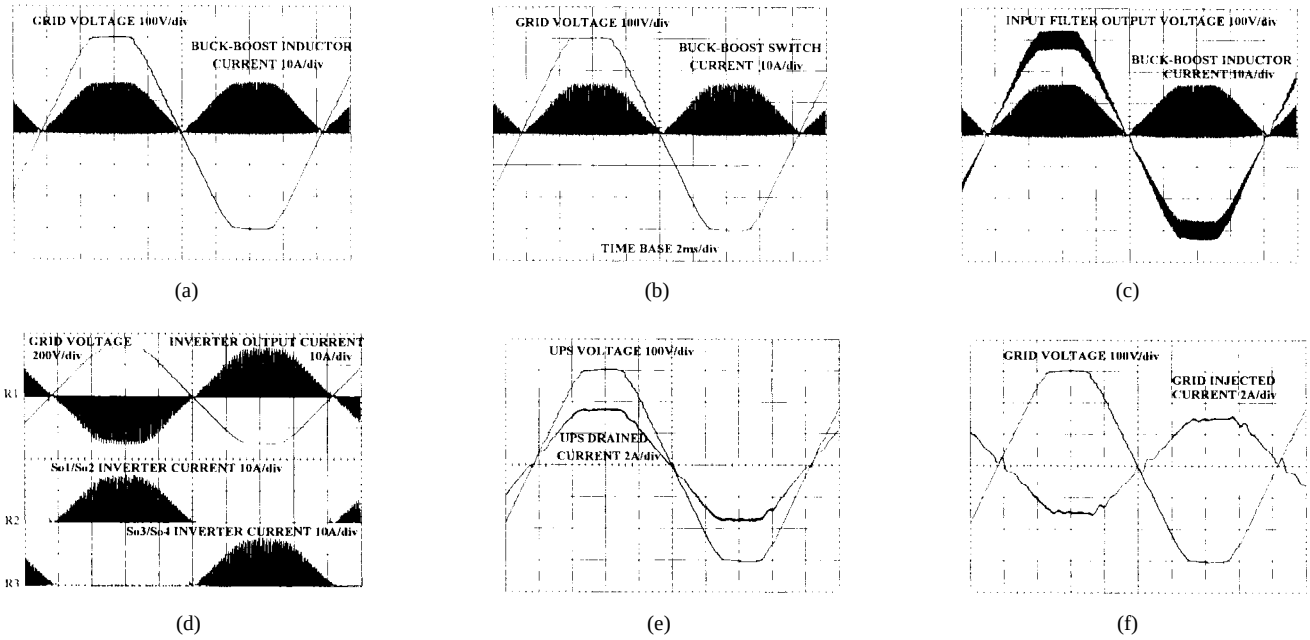

Fig. 12. Experimental results for DCM.

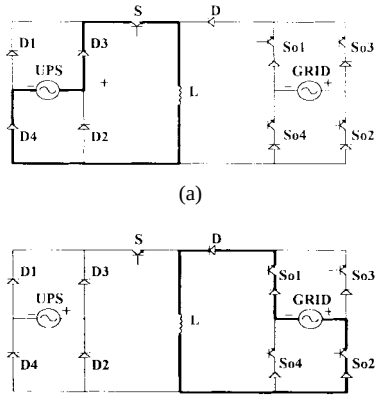

Fig. 13. Operation stages for a half period of the grid.

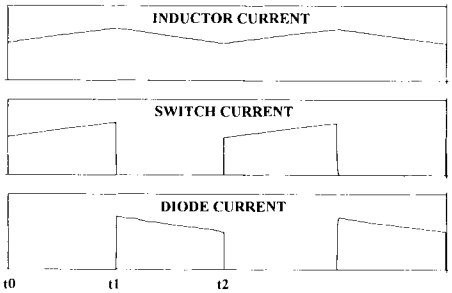

Fig. 14. Main-current waveforms in a switching period.

B. Control-Loop Analysis

In CCM, to obtain input and output sinusoidal currents in the power recycler, it is necessary to impose a sinusoidal current in the dc/dc converter inductor. So, using only one current loop, the power-recycler input and output currents present a sinusoidal waveform with low THD and high PF.

As the input and output voltages are established, the duty cycle is defined. Its value is almost constant, and there are only small variations in the duty cycle to follow the sinusoidal waveform in the inductor current.

In the buck converter, the output current flows through the inductor. As there is a relationship between the input and output current, as shown in (15), the resulting output current is also sinusoidal

$$I_i = DI_o. \tag{15}$$

In the boost converter, the inductor is placed at the input. The sinusoidal output current is assured by the relationship of

$$I_o = (1 - D)I_i. \tag{16}$$

In the buck–boost converter, by imposing a sinusoidal current in the inductor, the input and output currents will be sinusoidal due to the following relationships:

$$I_{in} = DI_L \tag{17}$$

$$I_o = (1 - D)I_L. \tag{18}$$

In the Cuk and sepic converters, the control is implemented in the input inductor current, and the output current will be sinusoidal according to the following relationship:

$$I_o = \frac{1 - D}{D} I_i. \tag{19}$$

For the zeta converter, the control is in the inductor connected to the switch. The relationships are presented in

$$I_i = D(I_L + I_o) \tag{20}$$

$$I_o = \frac{1 - D}{D} I_i. \tag{21}$$

To obtain the model of the current loop for the six basic topologies of the power recycler, the state-space average technique [7] was applied considering the switching period.

For the buck-converter topology, the transfer function for the inductor current in relation to the duty cycle is given in

$$\frac{I_L(S)}{D(S)} = \frac{V_{i_{av}}}{SL} \tag{22}$$

where

V_{iav} average value of the input voltage;
L dc/dc converter inductance.

The value of V_i varies in a sinusoidal way, and its average value was considered for the current-loop compensation.

Equation (23) considers the shunt resistor for current sampling and the pulse width modulation (PWM) sawtooth voltage

$$\frac{I_L(S)}{V_c(S)} = \frac{V_{i_{av}} R_{sh}}{SL_{V_{osc}}} \tag{23}$$

where

$V_c(S)$ error amplifier output voltage;
R_{sh} shunt resistor;
V_{osc} PWM sawtooth voltage, peak–peak.

Using the same method for the boost converter topology, one obtains

$$\frac{I_L(S)}{V_c(S)} = \frac{V_{o_{av}} R_{sh}}{SL_{V_{osc}}} \tag{24}$$

where

V_{oav} average value of the output voltage.

For the topologies using the buck–boost, Cuk, sepic, and zeta converters, the transfer function results

$$\frac{I_L(S)}{V_c(S)} = \frac{(V_{i_{av}} + V_{o_{av}})R_{sh}}{SL_{V_{osc}}}. \tag{25}$$

C. Simplified Design Example

To corroborate the theoretical analysis, a power recycler using the buck–boost converter was designed and implemented. Its characteristics are

$$V_i = 220 \text{ V}_{\text{rms}} \text{ (60 Hz)}$$
$$V_o = 220 \text{ V}_{\text{rms}} \text{ (60 Hz)}$$
$$P_i = 700 \text{ W}$$
$$f_s = 20 \text{ kHz}.$$

For the buck–boost topology, the duty cycle is given in

$$D = \frac{V_o}{V_i + V_o}. \tag{26}$$

In this case, the duty cycle results $D = 0.5$.

The buck–boost inductance is specified according to the maximum current ripple as denoted in

$$L = \frac{V_{i_p} D}{\Delta I_{L_{\max}} f_s} \tag{27}$$

where

$\Delta I_{L\,\max}$ maximum inductor-current ripple;
f_s switching frequency.

For a 3A-maximum inductor-current ripple in (27), we obtain $L = 2.59$ mH.

Using a shunt resistor of 0.1 Ω and $V_{osc} = 5.2$ V_{pp} in (25), the transfer function results

$$\frac{I_L(S)}{V_c(S)} = \frac{2940}{S}.$$

The compensator presented in [8] is adequate for this current loop. It has two poles (one placed at the origin to guarantee a small static error) and one zero. The crossing frequency was adjusted in 4.5 kHz.

D. Experimental Results

The implemented circuit is shown in Fig. 15, and the experimental results are presented in Fig. 16.

Only the current loop of the UC3854 (PF controller) was used. One can notice that a superposition in the drive signals of the current-inverter switches of ± 200 μs around the zero crossing of the grid voltage was used. The input and output filters were $C_{fi} = C_{fo} = 1$ μF and $L_{fi} = L_{fo} = 6.4$ mH. The grid voltage presented a THD of 3.5% and 226 V_{rms}. The UPS-drained current presented a THD of 9.5%—an angle of $+3.3^\circ$ with 715 W. The grid-injected current presented a THD of 8.6% and an angle of -6.5° with 636 W. The resulting efficiency was around 89%.

V. Extension to Other Topologies

One can extend this technique to the six basic dc/dc converters, as shown in Fig. 17. If the possible isolated dc/dc converter or other variations were used, many other topologies can be obtained.

It is important to notice that if the diodes of the switches of the current inverter are fast, the diode D of the dc/dc converter can be omitted without affecting the operation of

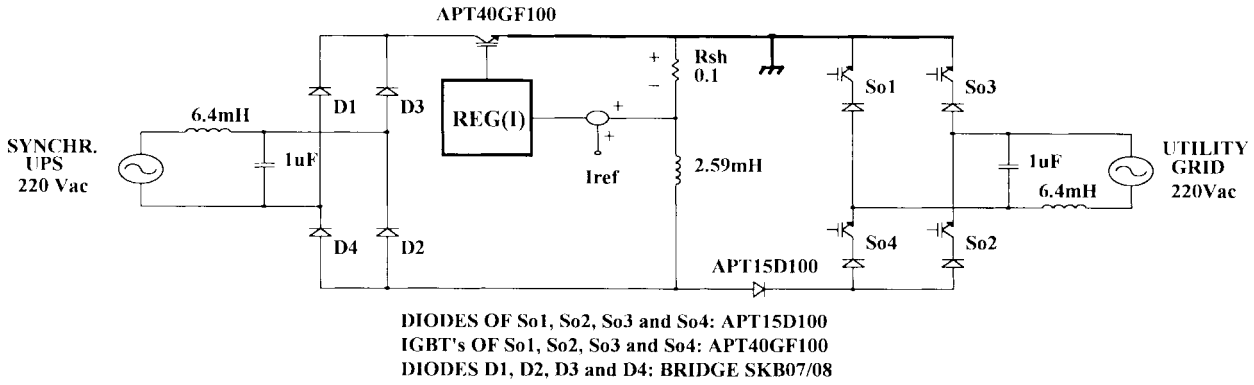

Fig. 15. Implemented circuit for CCM.

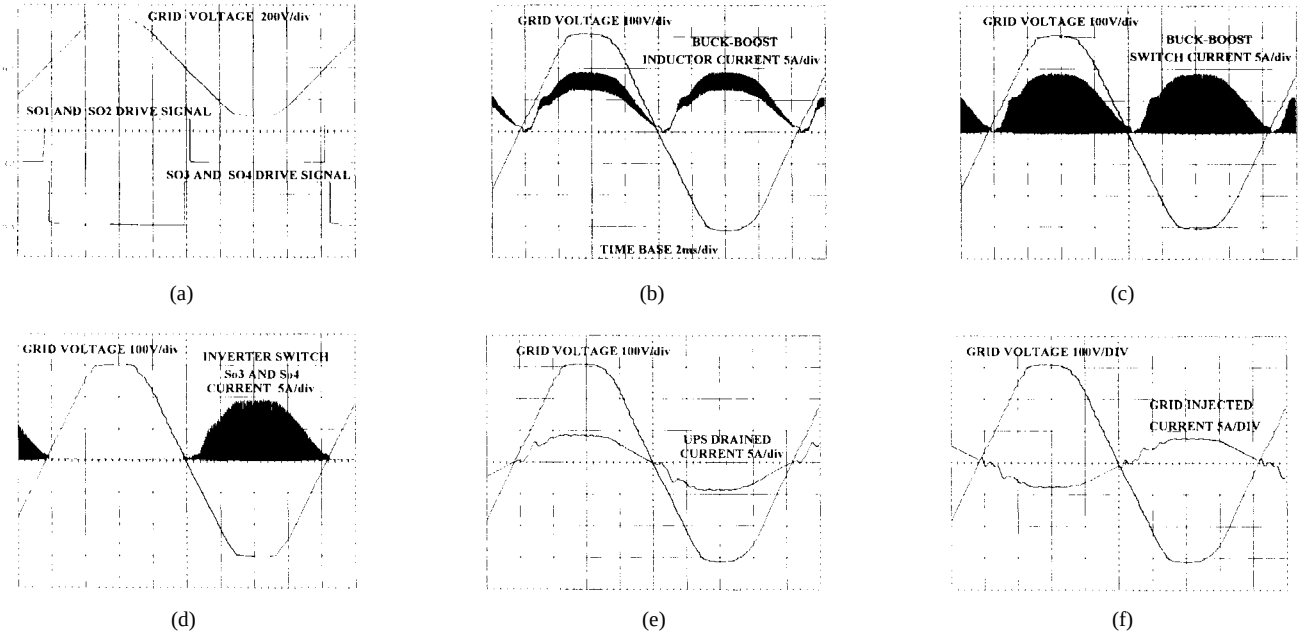

Fig. 16. Experimental results for CCM.

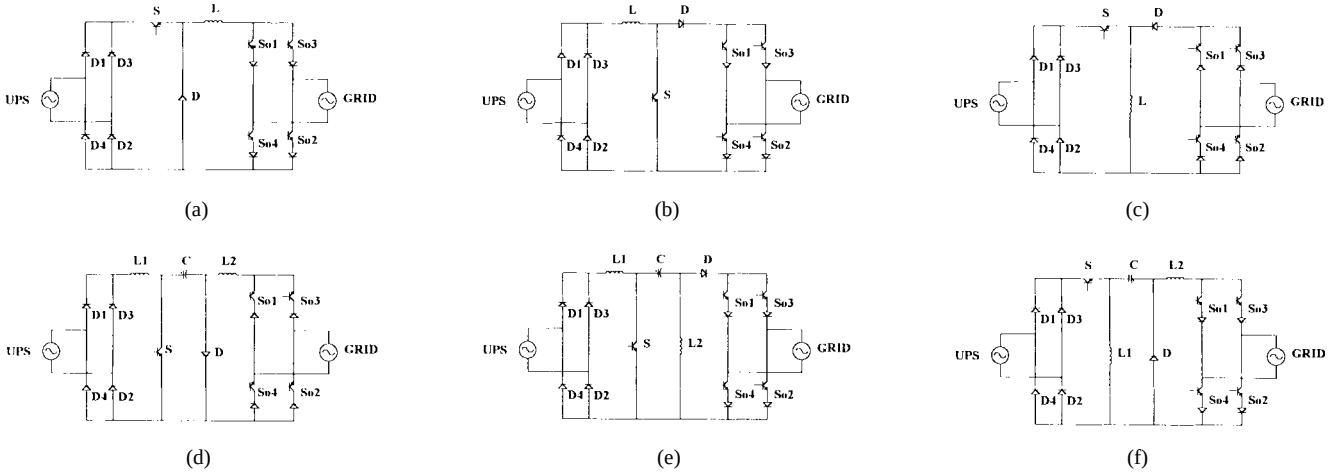

Fig. 17. The six basic topologies of the power recycler for synchronized UPS.

the power recycler in the case of the topologies using the boost, buck–boost, or sepic converters. However, if the diodes are not fast, the presence of diode D is obligatory.

Another way to reduce the current peak through the semiconductors of DCM is to utilize the interleaving technique: two dc/dc converters operating in DCM and shifted at 180°, each

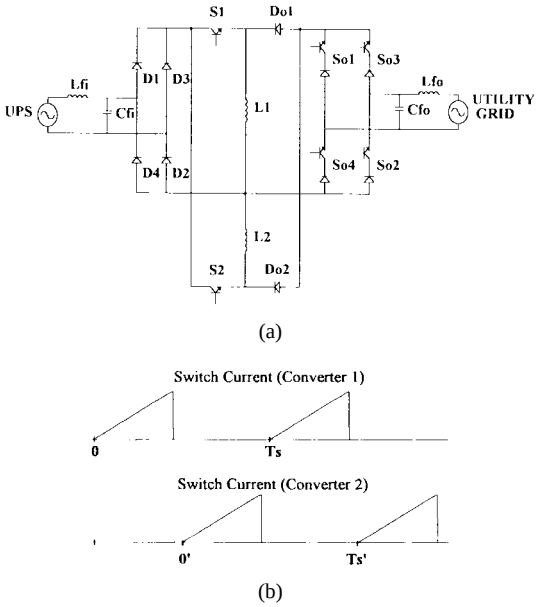

Fig. 18. Two converters operating in DCM 180° shifted.

one processing 50% of the total power. As a consequence, the current amplitude to be filtered will be halved and its frequency doubled. So, the filtering becomes easier and the volume of the filters is reduced.

Fig. 18 shows the circuit diagram for this case and the main waveforms.

VI. Conclusion

In this paper, we introduce and describe the operation of a family of converters intended to be used in the burn-in test of synchronized UPS's with sinusoidal voltage output. These converters replace the resistor load banks with the advantage that most of the electrical energy is sent back to the utility grid.

The economical benefits due to energy savings are evident and contribute in reducing the final price of the product.

The power-recycling concept is totally agreeable to the world concern about ecology and the optimized use of the available energy sources.

The most important characteristic of the proposed converters is their ability to drain from the UPS and to inject into the utility currents with low THD and high PF.

In DCM, the power recycler has the advantage of simplicity because it operates in an open loop. In CCM, we have lower current peak in the semiconductors, and the volume of the filters is reduced in comparison with DCM. Another important characteristic in this case is that by imposing a sinusoidal current in the dc/dc converter inductor, sinusoidal currents are obtained at the power-recycler input and output.

Mathematical analysis, design procedure, and experimental results for DCM and CCM operation are provided in this paper.

As the power recycler is connected to the utility grid, line disturbances, such as sags and surges, may affect its operation. So, some protection must be implemented to avoid these situations. The influence of the utility-grid frequency change is small since the UPS is synchronized, and the utility frequency variation is very reduced.

References

[1] G. A. O'Sullivan, "Power supplies testings with the power recycler," in *Proc. IEEE Power Conversion*, Sept. 1992, pp. 228–235.
[2] ———, "Power recycling: Safety and quality imperatives," in *Proc. IEEE Power Quality*, Sept. 1992, pp. 170–176.
[3] S. Gupta and V. Rangaswamy, "Load bank elimination for UPS testing," in *Proc. IEEE IAS*, 1990, pp. 1040–1043.
[4] J. F. Chen, C. L. Chu, T. H. Ai, and C. L. Huang, "The burn-in test of three-phase UPS by energy feedback method," in *Proc. IEEE PESC Rec.*, 1993, pp. 766–771.
[5] C. A. Ayres and I. Barbi, "A family of converters for power recycling during UPS's burn-in test," in *Proc. IEEE PESC Rec.*, 1995, pp. 486–492.
[6] ———, "CCM operation analysis of a family of converters for power recycling during the burn-in test of synchronized UPS's," in *Proc. IEEE PESC Rec.*, 1996, pp. 986–992.
[7] R. D. Middlebrook and S. Cuk, "A general unified approach to modeling switching converter power stages," in *Proc. IEEE PESC Rec.*, 1976, pp. 19–34.
[8] C. S. E. Silva, "Power factor correction with the UC3854," Application Note U-125, Unitrode Integrated Circuits Corporation.

Carlos Augusto Ayres (S'95) was born in Avaré, Sao Paulo, Brazil, in 1961. He received the B.S. and M.S. degrees in electrical engineering from the Federal Engineering School of Itajubá, Minas Gerais, Brazil, in 1984 and 1992, respectively. He is currently working toward the Ph.D. degree in electrical engineering at the Power Electronics Institute of Federal University of Santa Catarina, Florianópolis, Brazil.

In 1985, he joined the Department of Electronics of Federal Engineering School of Itajubá, where he is currently an Assistant Professor. His interests include dc/dc converters, PF correction, soft commutation, and energy conservation.

Ivo Barbi (M'78–SM'90) was born in Gaspar, Santa Catarina, Brazil, in 1949. He received the B.S. and M.S. degrees in electrical engineering from the Federal University of Santa Catarina, Florianópolis, Brazil, in 1973 and 1976, respectively, and the Ph.D. degree from the Institute National Polytechnique de Toulouse, Toulouse, France, in 1979.

He founded the Brazilian Power Electronics Society and the Power Electronics Institute of the Federal University of Santa Catarina. Currently, he is a Professor of the Power Electronics Institute.

Dr. Barbi has been an Associate Editor in the power converters area of the IEEE Transactions on Industrial Electronics since January 1992.